

Polyprenylated Benzoylphloroglucinols Isolated from *Garcinia* Species and Their Cytotoxic Effects on Cancer Cell Lines

Edwin R. Sukandar, Fadjar Mulya, Vudhichai Parasuk, Preecha Phuwapraisirisan, Kitiya Rassamee, Pongpun Siripong, and Sutin Kaennakam*



Cite This: *ACS Omega* 2024, 9, 43689–43696



Read Online

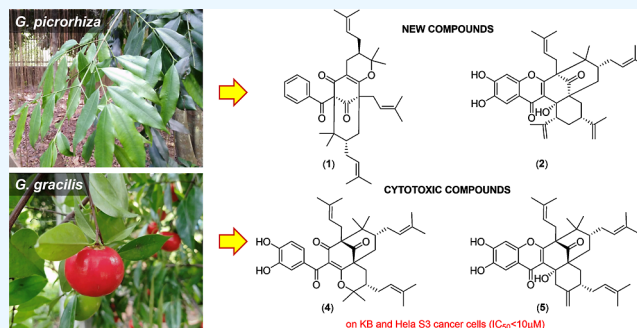
ACCESS |

Metrics & More

Article Recommendations

Supporting Information

ABSTRACT: Polyprenylated benzoylphloroglucinols (PPBPs) make up a group of complex natural products with anticancer potentials that are mainly distributed in *Garcinia* plants. As part of our intensive exploration on new bioactive substances from this genus, we report two undescribed PPBPs, picrorhizones I (1) and J (2), along with four known analogues (3–6) from the stem bark of *Garcinia picrorhiza* and *Garcinia gracilis*. The new structures were elucidated on the basis of spectroscopic analysis, particularly 1D and 2D NMR and HRESIMS, whereas the absolute configurations were determined by a combination of ECD and NMR calculations coupled with a DP4+ probability analysis. Being the least class in genus *Garcinia*, picrorhizone I possesses a type-A structure with the position of a benzoyl moiety attaching to one of the bridgehead carbons of a bicyclo[3.3.1]nonane skeleton, which differs from its major type-B counterparts. This work also represents the first report on the occurrence of PPBPs in *G. gracilis*. The cytotoxic evaluation of the isolated compounds revealed that isogarcinol (4) and garciyunnanin L (5) significantly inhibited the growth of KB and HeLa S3 cancer cells with IC_{50} values lower than $10 \mu\text{M}$, while 5 was also strongly active against the Hep G2 cancer cell line with an IC_{50} value of $8.02 \mu\text{M}$. Among the B-class derivatives bearing a lavandulyl side chain, cyclization of the moiety in the bicyclic phloroglucinol skeleton enhanced the cytotoxic properties on cancer cells.



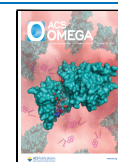
INTRODUCTION

The naturally occurring polyprenylated benzoylphloroglucinols (PPBPs), also known as polyprenylated benzophenones, can be found almost exclusively in plants belonging to the genus *Garcinia* (Clusiaceae) and *Hypericum* (Hypericaceae, which was previously considered to be a subfamily of Clusiaceae).¹ Over 500 PPBPs have been isolated from natural resources to date and recorded by the Grossmann group in an updated online database,² which are classified into type-A where the benzoyl group is attached to C-1 quaternary carbon and type-B which links the benzoyl part to C-2 of the keto–enol moiety in the phloroglucinol core structure. Not only this class of compounds possess diverse chemical architectures due to the modification or cyclization of prenyl side chains forming polycyclic structures but they also show potent biological properties, particularly anticancer effects.^{1,3} One of the notable examples is oblongifolin C, isolated from *Garcinia oblongifolia*, which was found to significantly suppress the growth of cancer cell lines in vitro by inducing apoptosis, inhibiting autophagy flux, and enhancing chemosensitivity of drug-resistant cells, as well as to reduce tumor metastasis in animal models.⁴

Garcinia plants are a prolific source of bioactive phenolic compounds covering xanthenes as their primary metabolites with relatively small structures to complex PPBP molecules.^{3,5,6}

During the course of a drug discovery project on Thai and Indonesian *Garcinia* species, two relevant medicinal plants were selected, including *Garcinia gracilis* Pierre and *Garcinia picrorhiza* Miq., due to their limited phytochemical information. Known as Cha-mang or Mak-paem in Thai, *G. gracilis* is an edible plant originally distributed to the Indochina region with its traditional use for fever remedy, while *G. picrorhiza* (local name: Kogbirat) is a woody plant native to Sulawesi and Maluku islands, Indonesia, and is formulated for wound healing treatment. Previous works from the aerial parts of *G. gracilis* revealed the presence of caged xanthenes, depsidones, and biphenyls with their anticancer properties, while our group previously studied the phytochemical contents of *G. picrorhiza* and purified a series of prenylated xanthenes and PPBPs bearing a rare cyclobutane-containing side chain with antiproliferative effects on several cancer cells and anti-inflammatory potentials.^{7–10} As our strong interest in

Received: June 29, 2024
Revised: October 5, 2024
Accepted: October 11, 2024
Published: October 16, 2024



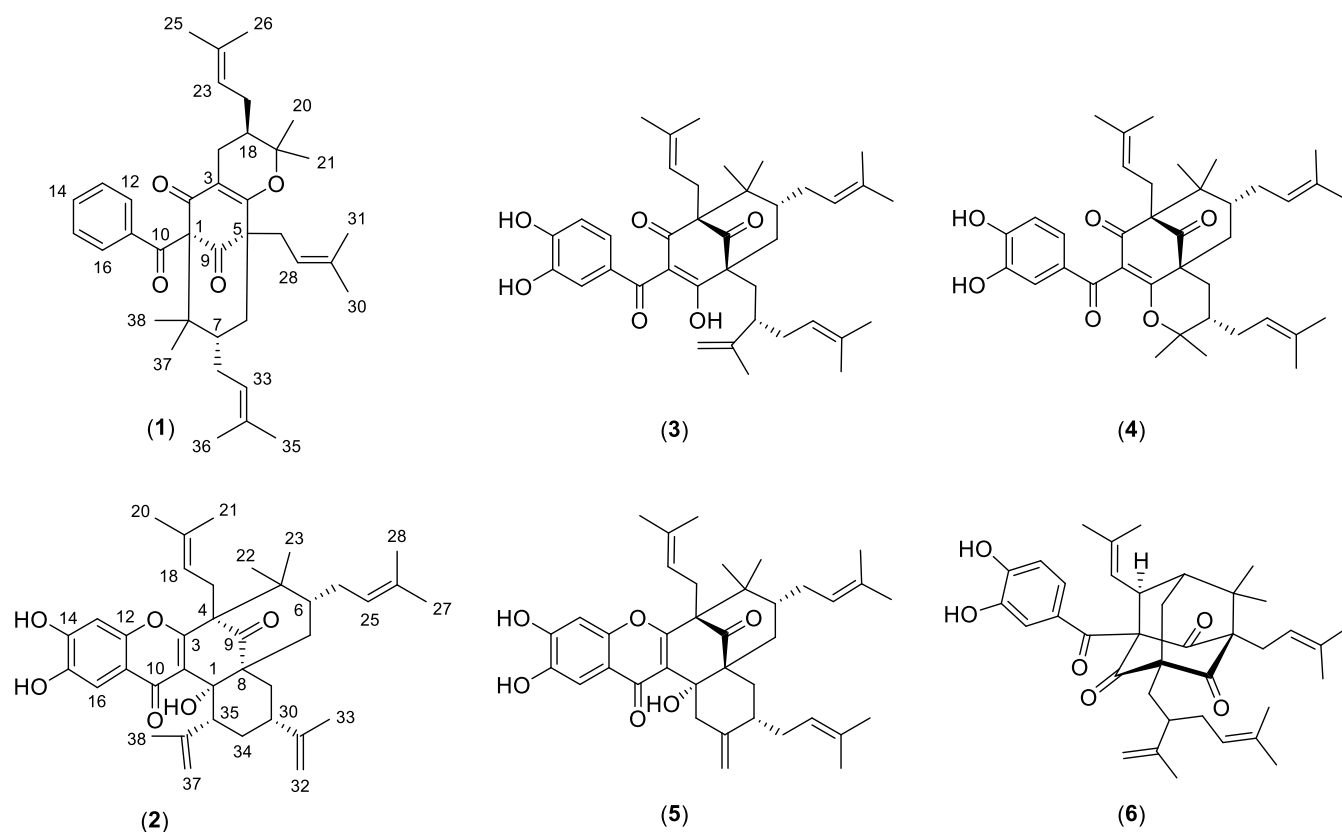


Figure 1. Polyprenylated benzoylphloroglucinols (1–6) isolated from the stem bark of *Garcinia picrorhiza* and *G. gracilis*.

searching novel bioactive PPBPs due to their intriguing molecular structures and having anticancer potentials, NMR-guided isolation was applied to target such secondary metabolites in the two *Garcinia* fractions, resulting in two new and four known derivatives being isolated. Herein, we report the isolation, structure elucidation, and cytotoxic evaluation of the isolated compounds against five human cancer cell lines.

RESULTS AND DISCUSSION

Structure Elucidation. From the CH_2Cl_2 -soluble fractions of *G. picrorhiza* and *G. gracilis*, two new PPBPs, picrorhizone I (1) and J (2), were isolated along with four known derivatives through a series of Chromatotron, silica gel, RP- C_{18} , and Sephadex LH-20 chromatographic separation. The known compounds were identified as garcinol (3),¹¹ isogarcinol (4),¹¹ garcyunnanin L (5),¹² and garciniagifolone A (6)¹³ after comparison of their ^1H and ^{13}C NMR spectra with the published data (Figure 1).

Compound 1 was isolated as a pale brown gum. Its molecular formula, $\text{C}_{38}\text{H}_{50}\text{O}_4$, was determined by HRESMS analysis of a sodium adduct ion at m/z 593.3592 [$\text{M} + \text{Na}$]⁺ (calcd for $\text{C}_{38}\text{H}_{50}\text{O}_4\text{Na}^+$, 593.3601), which equates to 14 degrees of unsaturation. The ^1H NMR spectrum showed resonances for five aromatic protons at δ_{H} 7.50 (each 1H, d, $J = 7.6$ Hz, H-12/H-16), 7.39 (1H, t, $J = 7.6$ Hz, H-14), and 7.26 (each 1H, t, $J = 7.6$ Hz, H-13/H-15) (Table 1). A contiguous spin system from H-12 to H-16 observed in the ^1H – ^1H COSY spectrum and HMBC correlations of H-12/H-16 to a carbonyl carbon C-10 (δ_{C} 193.5) constructed an unsubstituted benzoyl unit (Figure 2). The ^{13}C NMR and HSQC data assigned an isolated carbonyl carbon at δ_{C} 207.4

(C-9), a 1,3-keto–enol system at δ_{C} 192.0 (C-2), 168.9 (C-4), and 114.8 (C-3), three sp^3 quaternary carbons at δ_{C} 79.6 (C-1), 57.6 (C-5), and 48.4 (C-8), a methine at δ_{C} 44.3 (C-7), and a methylene at δ_{C} 40.5 (C-6), which were indicative of a benzoylphloroglucinol with a bicyclo[3.3.1]nonane-2,4,9-trione framework. In the HMBC spectrum, only *gem*-dimethyl protons at δ_{H} 1.12 (H-37) and 1.38 (H-38) correlated to the deshielded C-1, suggesting that 1 could be a type-A PPBP. Detailed NMR analysis of 1 showed that it was a derivative of propolone A,¹⁴ a metabolite obtained from Cuban propolis, where the key difference was the presence of additional signals corresponding to a prenyl unit in 1. These included a methine at $\delta_{\text{H}}/\delta_{\text{C}}$ 5.14 (t, $J = 7.0$ Hz, H-23)/121.7, a methylene at $\delta_{\text{H}}/\delta_{\text{C}}$ 2.25 (m, H-22a) and 1.82 (m, H-22b)/29.7, two methyls at $\delta_{\text{H}}/\delta_{\text{C}}$ 1.70 (s, H₃-25)/26.0 and 1.62 (s, H₃-26)/18.1, and a sp^2 quaternary carbon at δ_{C} 133.6 (C-24). The continuous COSY correlations of H₂-17/H-18/H₂-22/H-23 and the HMBC cross-peaks of H-22a/H-22b with C-17 (δ_{C} 22.4), C-18 (δ_{C} 41.3), and C-19 (δ_{C} 82.7) confirmed the position of the prenyl unit at C-18 (Figure 2).

^1H – ^1H coupling constant values and the NOESY experiment were used to determine the relative configuration of 1. The large coupling constant between H-6_{ax} and H-7 ($^3J_{6\text{ax},7} = \sim 13.0$ Hz) and NOE correlations of H-6_{eq}/H-7, H-6_{ax}/H-27_a, H-6_{ax}/H₃-37, and H₃-37/H-32_b favored axial placement for H-7 and equatorial positions for C-27 and C-32 in the chair conformation of the bridged bicyclic system and those allowed the benzoyl moiety at C-1 to be equatorially oriented (Figure 3a). The NOE cross-peak of H₃-20 and H-7 suggested an endo orientation of methyl CH₃-20. The diaxial orientation of H-17_b and H-18 was deduced from the coupling constant $J_{17\text{b},18} = 11.0$ Hz, which was supported by the lack of a NOE correlation

Table 1. ^1H (400 MHz) and ^{13}C (100 MHz) NMR Spectroscopic Data of **1** and **2** (δ in ppm)

position	1^a		position	2^b	
	δ_{H} (J in Hz)	δ_{C}		δ_{H} (J in Hz)	δ_{C}
1		79.6	1		81.8
2		192.0	2		121.7
3		114.8	3		165.5
4		168.9	4		62.3
5		57.6	5		50.9
6eq	1.95, dd (13.0, 4.2)	40.5	6	1.04 ^c	45.1
6ax	1.43, t (13.0)		7a	2.39, t (14.0)	41.8
7	1.60 ^c	44.3	7b	1.47, dd (14.0, 5.6)	
8		48.4	8		57.5
9		207.4	9		211.7
10		193.5	10		181.5
11		136.8	11		116.3
12	7.50, d (7.6)	128.6	12		146.4
13	7.26, t (7.6)	128.0	13	6.88, s	103.3
14	7.39, t (7.6)	132.0	14		154.7
15	7.26, t (7.6)	128.0	15		152.0
16	7.50, d (7.6)	128.6	16	7.29, s	108.5
17a	2.52, dd (17.0, 5.2)	22.4	17a	2.84, dd (14.0, 4.8)	28.1
17b	1.94, dd (17.0, 11.0)		17b	2.76, dd (14.0, 8.8)	
18	1.70 ^c	41.3	18	4.73, t (7.2)	121.0
19		82.7	19		135.6
20	1.17, s	20.3	20	1.46, s	26.4
21	1.48, s	27.4	21	1.71, s	18.5
22a	2.25, brdt (14.0, 4.8)	29.7	22	0.94, s	20.1
22b	1.82, dd (14.0, 8.4)		23	1.02, s	25.5
23	5.14, t (7.0)	121.7	24a	1.97, brd (10.0)	29.8
24		133.6	24b	1.59, dd (10.0, 4.0)	
25	1.70, s	26.0	25	4.96, t (7.2)	124.2
26	1.62, s	18.1	26		134.3
27a	2.54, dd (14.0, 6.0)	29.0	27	1.68, s	25.9
27b	2.43, dd (14.0, 7.2)		28	1.53, s	18.0
28	5.03, t (6.8)	119.5	29ax	1.96, dd (12.4, 4.0)	34.9
29		134.2	29eq	1.48, t (12.4)	
30	1.67, s	26.2	30	2.76, td (12.4, 4.4)	40.8
31	1.65, s	18.4	31		151.2
32a	2.16, dd (13.4, 5.8)	26.9	32a	4.80, s	109.2
32b	1.69 ^c		32b	4.75, s	
33	4.98, t (6.8)	122.9	33	1.79, s	21.0
34		133.4	34ax	2.07, q (12.4)	32.3
35	1.67, s	25.9	34eq	1.36, d (12.4)	
36	1.57, s	17.9	35	1.79 ^c	57.4
37	1.12, s	16.0	36		148.1
38	1.38, s	23.8	37a	4.48, s	114.3
			37b	4.28, s	
			38	1.73, s	21.7

^aRecorded in CDCl_3 , ^bRecorded in methanol- d_4 , ^cOverlapping signals and the data are deduced from HSQC or HMBC spectra.

between the two protons. In order to confirm the absolute configuration, ECD calculations were carried out on two possible enantiomers of **1**: (1*S*,5*S*,7*S*,18*R*)-**1** and (1*R*,5*R*,7*R*,18*S*)-*ent*-**1**. Conformers for each model with Boltzmann populations higher than 1% were selected for subsequent TDDFT-ECD calculation at the B3LYP/6-31++G(d,p) level to obtain the averaged spectrum, as shown in Figure 3b. The computed ECD data of (1*S*,5*S*,7*S*,18*R*)-**1** were the best fit with that of the experimental ECD spectrum, and the absolute configuration was determined consequently.

Compound **2** was isolated as brown gum with a molecular formula of $\text{C}_{38}\text{H}_{48}\text{O}_6$, as deduced from its protonated molecular ion at m/z 601.3527 $[\text{M} + \text{H}]^+$ (calcd for $\text{C}_{38}\text{H}_{49}\text{O}_6^+$, 601.3524) in the HRESIMS analysis. Two aromatic protons at δ_{H} 7.29 (s, H-16)/ δ_{C} 108.5 and δ_{H} 6.88 (s, H-13)/ δ_{C} 103.3 were assigned in the 1D NMR and HSQC data. The HMBC data revealed cross-peaks of H-13 with quaternary carbons C-11 (δ_{C} 116.3), C-12 (δ_{C} 146.4), C-14 (δ_{C} 154.7), C-15 (δ_{C} 152.0), and H-16 with conjugated carbonyl carbon C-10 (δ_{C} 181.5), C-12, C-14, and C-15, which indicated a 2,4,5-trioxygenated benzoyl moiety (Figure 2). The ^{13}C NMR resonances corresponding to a carbonyl carbon at δ_{C} 211.7 (C-9), an enolic system at δ_{C} 165.5 (C-3) and 121.7 (C-2), four sp^3 quaternary carbons at δ_{C} 81.8 (C-1), 62.3 (C-4), 50.9 (C-5), and 57.5 (C-8), a methine at δ_{C} 45.1 (C-6), and a methylene at δ_{C} 41.8 (C-7) were once again associated with a bicyclo[3.3.1]nonane skeleton in the PPBP structure of **2** (Table 1). The above analysis, together with a detail comparison of the NMR data of **2** and garcinoxanthocin **A**,¹⁵ reinforced the construction of a benzoylphloroglucinol in which one oxygen of the keto–enol system was connected to C-12 of the benzoyl ring. A continuous spin system of H-29/H-30/H-34/H-35 observed in the COSY spectrum and the HMBC correlations of H-29 to C-1, C-8, and C-9 and H-34 to C-1 completed the assignment of the six-membered ring positioned at C-1 and C-8 in the bicyclic ring of **2** (Figure 2). Two propylene moieties at C-30 and C-35 were deduced by the resonances for two terminal olefinic protons at δ_{H} 4.80 and 4.75 (each 1H, s, H-32a, and H-32b)/ δ_{C} 109.2 and 4.48 and 4.28 (each 1H, s, H-37a, and H-37b)/ δ_{C} 114.3, two sp^2 quaternary carbons at δ_{C} 151.2 (C-31) and 148.1 (C-36), and the HMBC correlations of methyl H-33 to C-30, C-31, and C-32 and methyl H-38 to C-35, C-36, and C-37.

The diaxial coupling constant between H-6 and H-7ax ($^3J_{6,7ax} = 14.0$ Hz) and NOE correlations of H-17a/H-23, H-23/H-24a, H-22/H-7ax, and H-6/H-7eq were observed in **2**, suggesting the equatorial orientation of C-17 and C-24 in a chair conformation of the bicyclic part (Figure 3a). Meanwhile, a quartet proton H-34ax with an J value of 12.4 Hz suggested that this proton was flanked by two adjacent axial protons H-30 and H-35 and required itself to be axially oriented in a chair conformation of the cyclohexane moiety, which was further supported by the 1,3-diaxial interactions of H-29ax/H-34ax and H-30/H-35 in the NOESY spectrum. The NOE correlation between H-35 and H-7eq allowed methines H-30 and H-35 to be pointed toward the endo side of the bicyclic ring. Since the relative configuration at C-1 could not be defined by the NOESY data, the theoretical NMR/DP4+ analysis was performed on model (1*S*,4*R*,6*R*,8*R*,30*R*,35*R*)-**2a** and its diastereomer (1*R*,4*R*,6*R*,8*R*,30*R*,35*R*)-**2b**. The DP4+ statistical results indicated the predominance of the 1*S* isomer in **2a** with a probability of 100% in all H and C data (Table S1). The absolute configuration of **2** was determined as

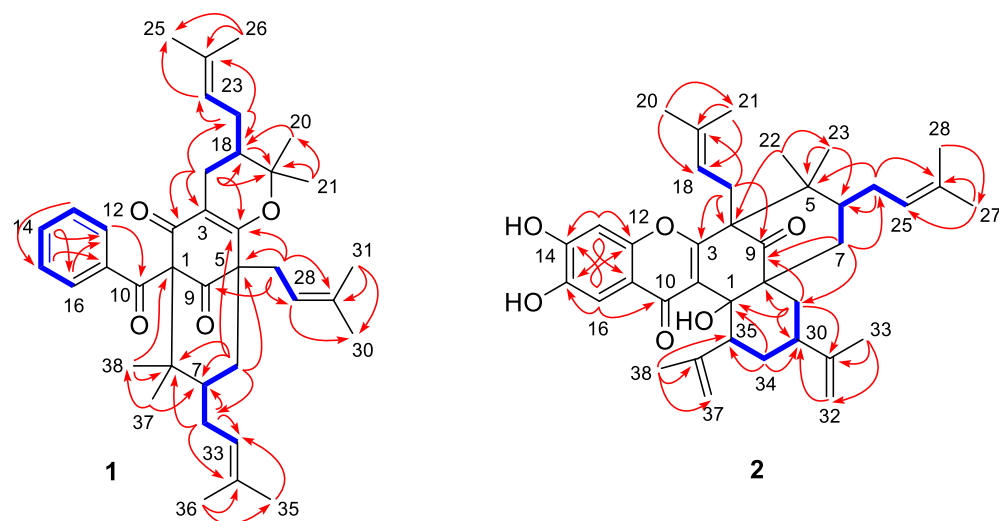
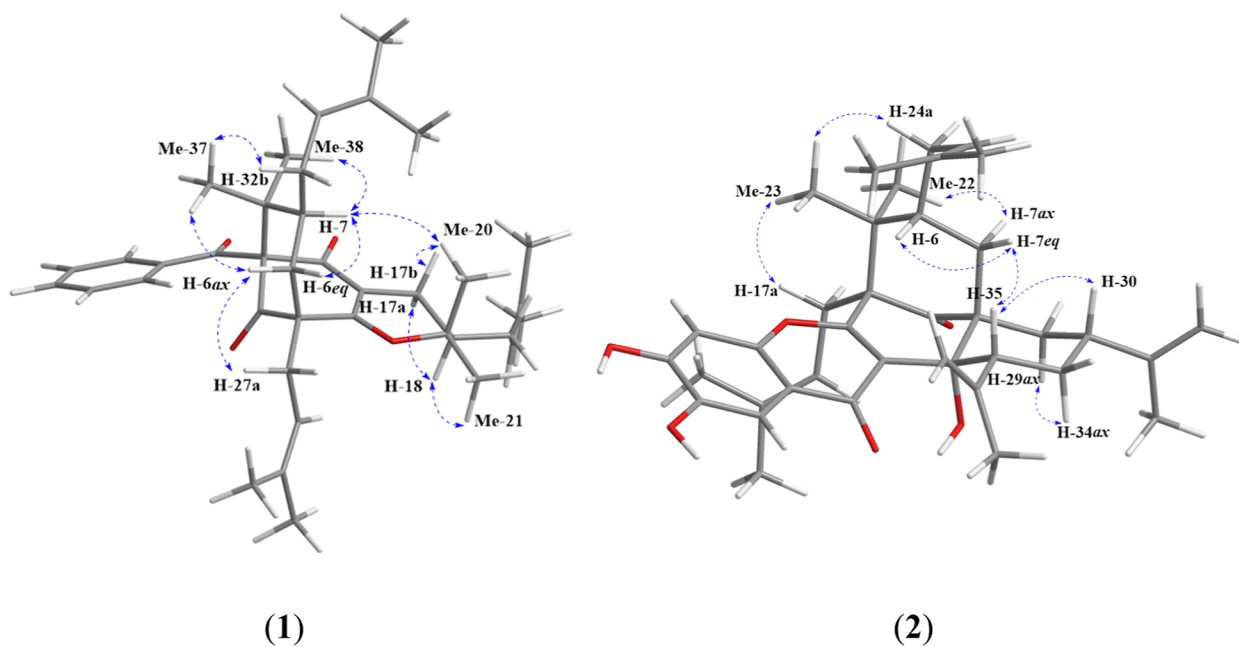


Figure 2. Key COSY and HMBC correlations of compounds **1** and **2**.

(a)



(b)

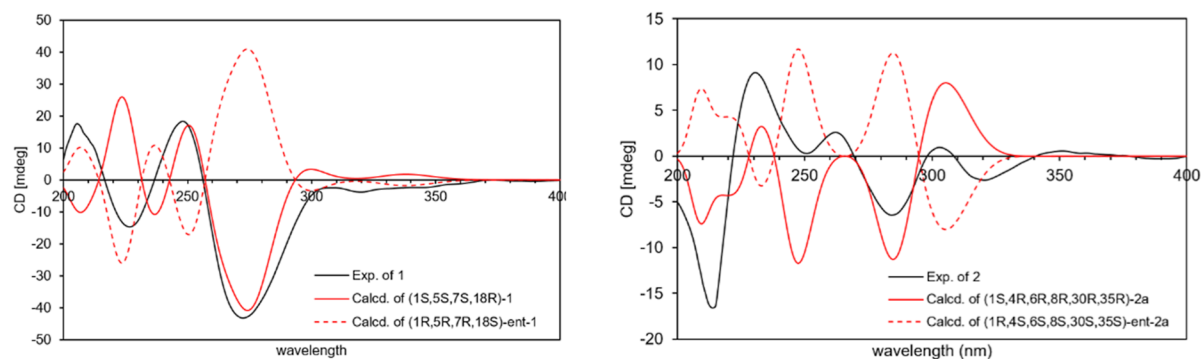


Figure 3. (a) Selected NOESY correlations of **1** and **2**. (b) Experimental and calculated ECD spectra of **1** and **2**.

(1*S*,4*R*,6*R*,8*R*,30*R*,35*R*) according to the similarity of the experimental ECD spectrum of **2** with that of the calculated ECD spectrum of **2a**, as shown in Figure 3b.

No less than 250 PPBPs present in various *Garcinia* plants, with the majority falling into type-B structures. A few numbers

of type-A derivatives, including picrorhizone I (**1**), were discovered in this genus with *Garcinia multiflora* and *Garcinia subelliptica* as the main producers, whereas their abundance were previously recognized in *Hypericum* genera with common structures containing nonaromatic acyl groups (e.g., isopropyl

Table 2. Cytotoxic Activity^a of Isolated Compounds (1–6) Against Five Human Cancer Cell Lines

compound	IC ₅₀ ± SD (μM)				
	KB	Hela S3	MCF-7	Hep G2	HT-29
1	20.71 ± 2.24	26.29 ± 1.65	NT	NT	NT
2	21.71 ± 0.75	31.45 ± 0.21	NT	NT	NT
3	18.27 ± 2.11	26.74 ± 0.92	NT	NT	NT
4	5.39 ± 0.49	9.27 ± 1.08	19.72 ± 1.73	35.38 ± 2.17	45.76 ± 1.84
5	2.37 ± 0.69	4.72 ± 1.02	15.39 ± 1.28	8.02 ± 0.74	16.74 ± 0.28
6	13.48 ± 1.27	19.78 ± 0.76	NT	NT	NT
Doxorubicin ^b	0.02 ± 0.01	0.15 ± 0.02	1.29 ± 0.02	1.00 ± 0.17	0.59 ± 0.03

^aResults are expressed as means ± SD of three replicates. ^bDoxorubicin was used as the positive control. ^cNote: IC₅₀ ≤ 10 μM = good cytotoxicity, 10 μM < IC₅₀ ≤ 50 μM = moderate cytotoxicity, 50 μM < IC₅₀ ≤ 100 μM = weak activity, IC₅₀ > 100 μM = not active, and NT = not tested.

and *s*-butyl).² Within the B-class, picrorhizone J (2) and garciyunnanin L (5) were biosynthesized via oxidative cyclization of the enol moiety at C-3 to the C-12 of benzoyl group, which form a xanthone-like structure,¹⁶ while C–C bond formation between the C-24 prenyl side chain and C-2 in garcinol (3) generates a tricyclic adamantane skeleton as in garciniagifolone A (6).¹⁷

Cytotoxic Assay. In vitro cytotoxic screening of the isolated compounds (1–6) was initially conducted using the MTT assay on KB and Hela S3 cancer cells. The tested samples showing an IC₅₀ value lower than 10 μM against the two cell lines were further evaluated on their inhibitory effects against the other three cancer cell lines, including MCF-7, Hep G2, and HT-29, as described in Table 2. The cyclization of lavandulyl functionality at C-8, forming a six-membered ring as in isogarcinol (4), could enhance the cytotoxic effects against KB and Hela S3 cell lines with IC₅₀ values ~3-fold lower than those containing the free side chain as in garcinol (3). Another compound having the similar pattern, garciyunnanin L (5), also significantly suppressed the growth of three human cancer cells (KB, Hela S3, and Hep G2) with IC₅₀ values ranging from 2.37–8.02 μM.

Previous reports revealed that the cyclized PPBP derivatives as in isoxanthochymol, xanthochymusones D, E, and I were active against a panel of human cancer cells, including A549, B16, Huh-7, and Hep 3B with IC₅₀ values lower than 25 μM, while a decreased cytotoxic effect was observed in its analogue, xanthochymol, bearing a free lavandulyl moiety at C-8.^{18,19} Not only having anticancer activities, the cyclic products of 7-*epi*-garcinol were found to be significantly active as antimalarial agents against the FcB1 strain of *Plasmodium falciparum* with IC₅₀ values up to ~5-fold better than its ring-opening form.²⁰ These initial findings provide insight for the structure modification of PPBPs with the main focus on the cyclization of side chains to the ketol-enol moiety to further understand their structure–activity relationships.

CONCLUSIONS

Two new PPBPs, picrorhizones I (1) and J (2), from the stem bark of *G. picrorhiza* and four known derivatives, including garcinol (3), isogarcinol (4), garciyunnanin L (5), and garciniagifolone A (6), from the stem bark of *G. gracilis* were isolated. The discovery of the minor group of type-A PPBPs in *Garcinia* plants, including picrorhizone I, could enrich the phytochemical diversity of the genus which differ to those present in other genera, such as *Hypericum* with the majority containing aliphatic acyl moieties. The potent antiproliferative properties of isogarcinol and garciyunnanin L against KB and

Hela S3 cancer cell lines (IC₅₀ < 10 μM) prompt for further studies in detailed mechanisms in action.

METHODS

General Experimental Procedures. Optical rotations were measured on a JASCO P-1010 polarimeter (JASCO Corporation, Easton, MD, USA). The IR data were obtained on a Nicolet 6700 FT-IR spectrometer using the KBr disk method (Thermo Fisher Scientific, Waltham, MA, USA). The experimental ECD data were recorded on a JASCO Model J-815 spectropolarimeter (JASCO Corporation). The NMR spectra were acquired on a Bruker 400 AVANCE (Bruker, Rheinstetten, Germany) and a JEOL JNM-ECZ500 R/S1 (JEOL Ltd., Tokyo, Japan) NMR spectrometer in CDCl₃ and methanol-*d*₄ (Merck, Darmstadt, Germany). The HRMS spectra were recorded using a Bruker MICROTOF model mass spectrometer (Bruker, Billerica, MA, USA). Silica gel (70:230 mesh, Merck, Darmstadt, Germany), Sephadex LH-20 (25:100 mm, GE Healthcare Bio-Sciences AB, Uppsala, Sweden), and Chromatorex ODS/RP-C₁₈ (100:200 mesh; Fuji Silysia Chemical Ltd., Tokyo, Japan) were used for column chromatography. Radial chromatography (Chromatotron model 7924 T, Harrison Research, Palo Alto, California, USA) was carried out on silica gel 60 GF₂₅₄ containing gypsum (Merck).

Plant Material. The stem bark of *G. picrorhiza* was collected in Bogor Botanical Garden, Bogor, Indonesia (6°35'51" S 106°47'55" E) in July 2006. The plant material was identified by Dr. Rismita Sari, and a voucher specimen (no. VIA.26) was deposited at Bogor Botanical Garden, Indonesia. The stem bark of *G. gracilis* was purchased from Saraburi Province, Thailand (14°30'53" N 100°54'32" E) in April 2018. The plant authentication was conducted by comparing the sample with a voucher specimen (GG-022554) deposited at the Faculty of Pharmaceutical Sciences, Chulalongkorn University, Thailand.

Extraction and Isolation. The extraction of *G. picrorhiza* stem bark and liquid–liquid partition of the MeOH crude extract using CH₂Cl₂ and EtOAc was in accordance to the previous procedure.¹⁰ The silica gel column chromatographic fractionation of the CH₂Cl₂-soluble fraction (54.1 g) was performed with hexanes/EtOAc (95:5–0:100) to obtain fractions A–R. Fraction C (327.0 mg) was subjected to a Sephadex LH-20 column with CH₂Cl₂/MeOH (50:50) to yield subfractions C1–C3. Subfraction C2 (102.6 mg) was then chromatographed on a silica gel column eluted with hexanes/CH₂Cl₂ (75:25) to obtain subfractions C2.1–C2.3. Compound 1 (5.8 mg) was purified from the last subfraction (44.2 mg) by a Chromatotron using hexanes/EtOAc (95:5).

Fraction Q (3.3 g) was separated using a silica gel column eluted with a gradient elution of hexanes/EtOAc (75:25–20:80) to give three subfractions (Q1–Q3). Compound 2 (5.3 mg) was obtained from the purification of subfraction Q1 (98.2 mg) using a RP-C₁₈ column using an eluent system of MeOH/H₂O (80:20).

The extraction of *G. gracilis* stem bark (5.0 kg) was performed at room temperature using MeOH (20 L each for 3 days). The crude extract obtained after solvent removal was suspended in distilled water and applied to the liquid–liquid partition by CH₂Cl₂ and EtOAc. The CH₂Cl₂-soluble fraction (300.0 g) was subjected to a silica gel column with hexanes/EtOAc (100:0–0:100) to generate 12 fractions (A–L). Fraction C (4.8 g) was loaded into a Sephadex LH-20 column with CH₂Cl₂/MeOH (50:50) to give subfractions C1–C3, by which subfraction C1 (1.6 g) was rechromatographed using the same technique and solvent system to afford four subfractions (C1.1–C1.4). Purification of subfraction C1.1 (356.1 mg) by an RP-C₁₈ column with an isocratic system of MeCN/H₂O (80:20) gave compound 3 (52.7 mg). Subfraction C1.2 (508.4 mg) was loaded into an RP-C₁₈ column eluted with MeCN/H₂O (80:20) to yield subfractions C1.2.1–C1.2.7. Subfraction C1.2.2 (37.6 mg) was further purified by a Chromatotron using an eluent mixture of hexanes/EtOAc (70:30) to afford compound 6 (3.1 mg). Subfraction D (2.9 g) was fractionated by a Sephadex LH-20 column with CH₂Cl₂/MeOH (50:50) to provide subfractions D1–6, in which compound 4 (19.5 mg) was obtained as a precipitate from subfraction D2. Separation of fraction E (6.4 g) was conducted using a Sephadex LH-20 column with CH₂Cl₂:MeOH (50:50) to give seven subfractions (E1–E7). Subfraction E2 (672.3 mg) was further subjected on an RP-C₁₈ column eluted with MeOH/H₂O (80:20) to obtain subfractions E2.1–E2.3, and compound 5 (8.4 mg) was purified from subfraction E2.3 (89.0 mg) by a Chromatotron with an isocratic system of hexanes/EtOAc (70:30).

Picrorrhizone I (1). Pale brown gum; $[\alpha]_D^{20}$ –45.0 (*c* 0.10, CHCl₃); ECD (*c* 0.001, MeOH) λ_{\max} ($\Delta\epsilon$) 207 (+16.5), 227 (–14.7), 250 (+17.3), 274 (–43.0), 304 (–2.8), 321 (–3.8) nm; IR ν_{\max} (KBr): 3435, 2928, 1720, 1599, 1375, 1224 cm^{–1}; ¹H (400 MHz, CDCl₃) and ¹³C NMR (100 MHz, CDCl₃) spectroscopic data, see Table 1; and HRESIMS *m/z* 593.3592 [M + Na]⁺ (calcd for C₃₈H₅₀O₄Na⁺, 593.3601).

Picrorrhizone J (2). Brown gum; $[\alpha]_D^{20}$ –6.3 (*c* 0.07, MeOH); ECD (*c* 0.001, MeOH) λ_{\max} ($\Delta\epsilon$) 214 (–16.6), 233 (+8.6), 251 (+0.3), 264 (+2.4), 286 (–6.3), 305 (+0.8), 322 (–2.6), 350 (+0.6) nm; IR ν_{\max} (KBr): 3385, 2972, 1721, 1621, 1474, 1376, 1292 cm^{–1}; ¹H (400 MHz, methanol-*d*₄) and ¹³C NMR (100 MHz, methanol-*d*₄) spectroscopic data, see Table 1; and HRESIMS *m/z* 601.3527 [M + H]⁺ (calcd for C₃₈H₄₉O₆⁺, 601.3524).

ECD and NMR Chemical Shift Calculations. Conformational analysis of 1 and 2 were carried out using Molecular Operating Environment (MOE) software under MMFF94 molecular mechanics force field with Monte Carlo searching.²¹ The lowest-energy conformers contributing to more than 1.0% of the Boltzmann population were optimized by density functional theory (DFT) at the B3LYP/6-31++G(d,p) level of theory. Time-dependent (TD)-DFT B3LYP/6-31++G(d,p) incorporating polarizable continuum model (PCM) with methanol as a solvent and *n* states = 50 was performed for ECD calculation. The theoretical ECD spectra obtained were visualized using SpecDis 1.71 with σ = 0.2.²² The final spectra

were generated according to the Boltzmann weighting of each conformer. The NMR chemical shift calculations using the gauge-including atomic orbital (GIAO) method were performed at the B3LYP/6-31++G(d,p) level, and frequency analysis was carried out at the same theoretical level to confirm that there were no imaginary frequencies. The calculated shielding tensors were subjected to DP4+ probability measure by weighing the Boltzmann distribution rate²³ and a multistandard method was used to determine the chemical changes.^{24,25} Methanol and benzene were used as references for calculating the chemical shifts of sp³- and sp²-hybridized carbon atoms, respectively. The DFT, TD-DFT, and GIAO NMR calculations were carried out using Gaussian16 program.²⁶

Cytotoxicity Assay. The cytotoxic evaluation of compounds 1–6 was performed by the MTT colorimetric method against human epidermoid carcinoma (KB), cervical carcinoma (HeLa S3), breast adenocarcinoma (MCF-7), hepatocellular carcinoma (Hep G2), and colon adenocarcinoma (HT-29) following the previous protocol.⁹ The cells were maintained in minimum essential medium Eagle, supplemented with 10% fetal bovine serum, 100 U/mL penicillin, and 100 μg/mL streptomycin sulfate (Gibco, Rockville, MD, USA) at 37 °C in an atmosphere of 5% CO₂. The cell aliquots were seeded in 96-well plates (3000 cells/well) and incubated for 24 h. The cells were then treated with different concentrations of the tested compounds (0.3–100 μM) and further incubated with the same condition. After a 72 h incubation, the cells were washed with PBS, and 20 μL of MTT solution (5 mg/mL in PBS, Sigma, St. Louis, MI, USA) was added to each well with additional incubation of 3 h. The supernatant was decanted and mixed with DMSO (100 μL per well). The formazan formation was determined colorimetrically at 550 nm by a microplate reader (Tecan Trading AG, Switzerland). Control cells were treated with 0.1% DMSO and doxorubicin was used as a positive control. The data obtained represent mean ± SD from three experiments.

■ ASSOCIATED CONTENT

Supporting Information

The Supporting Information is available free of charge at <https://pubs.acs.org/doi/10.1021/acsomega.4c06030>.

1D and 2D NMR spectra, HRMS spectra, IR spectra, DFT-optimized structures of dominant conformers of 1 and 2, and DP4+ probability results for 2a and 2b (PDF)

■ AUTHOR INFORMATION

Corresponding Author

Sutin Kaennakam – Department of Agro-Industrial, Food, and Environmental Technology, Faculty of Applied Science, King Mongkut's University of Technology North Bangkok (KMUTNB), Bangkok 10800, Thailand; orcid.org/0000-0003-1938-035X; Phone: +66 2555 2000-24 ext. 4702; Email: sutin.k@sci.kmutnb.ac.th

Authors

Edwin R. Sukandar – Department of Agro-Industrial, Food, and Environmental Technology, Faculty of Applied Science, King Mongkut's University of Technology North Bangkok (KMUTNB), Bangkok 10800, Thailand; Department of

Chemistry, Faculty of Mathematics and Natural Sciences, Bandung Institute of Technology, Bandung 40132, Indonesia

Fadjar Mulya – Nanotechnology Engineering, Faculty of Advanced Technology and Multidiscipline, Universitas Airlangga, Surabaya 60115, Indonesia

Vudhichai Parasuk – Department of Chemistry, Faculty of Science, Chulalongkorn University, Bangkok 10330, Thailand; orcid.org/0000-0001-9265-6135

Preecha Phuwapraisrisan – Department of Chemistry, Faculty of Science, Chulalongkorn University, Bangkok 10330, Thailand; orcid.org/0000-0001-6481-7712

Kitiya Rassamee – Natural Products Research Section, Research Division, National Cancer Institute, Bangkok 10400, Thailand

Pongpun Siripong – Natural Products Research Section, Research Division, National Cancer Institute, Bangkok 10400, Thailand

Complete contact information is available at:

<https://pubs.acs.org/10.1021/acsomega.4c06030>

Author Contributions

E.R.S.: Conceptualization, Investigation, Formal analysis, Writing—Original Draft; F.M. and K.R.: Investigation, Formal analysis; V.P., P.P., and P.S.: Supervision, Validation, Writing—Review & Editing; S.K.: Conceptualization, Project administration, Funding acquisition, Supervision, Writing—Review & Editing. All authors have read and agreed to the manuscript.

Notes

The authors declare no competing financial interest.

ACKNOWLEDGMENTS

This research budget was allocated by National Science, Research and Innovation Fund (NSRF) and King Mongkut's University of Technology North Bangkok (Project no. KMUTNB-FF-67-B-37). The Science and Technology Research Institute of KMUTNB is acknowledged for a postdoctoral research fellowship (Grant no. KMUTNB-Post-67-11) to E.R.S. The authors thank Prof. Santi Tip-pyang (CU, Thailand) and Prof. Taslim Ersam (ITS, Indonesia) for lab facility in plant extraction and useful discussions, as well as with Dr. Thi-Kim-Dung Le (TDTU, Vietnam) for technical support in computational analysis. F.M. and V.P. are grateful for computational resources supported by the Center of Excellence in Computational Chemistry (CECC), Department of Chemistry, Chulalongkorn University.

REFERENCES

- (1) Yang, X. W.; Grossman, R. B.; Xu, G. Research progress of polycyclic polyprenylated acylphloroglucinols. *Chem. Rev.* **2018**, *118*, 3508–3558.
- (2) Grossman, R. B. Table of naturally occurring PPAPs. ACS Division of Organic Chemistry. 2024. <https://organicchemistrydata.org/grossman/ppap/allPPAPs.html> (accessed Jun 14 2024)
- (3) Phang, Y.; Wang, X.; Lu, Y.; Fu, W.; Zheng, C.; Xu, H. Bicyclic polyprenylated acylphloroglucinols and their derivatives: structural modification, structure-activity relationship, biological activity and mechanism of action. *Eur. J. Med. Chem.* **2020**, *205*, 112646.
- (4) Bailly, C.; Vergoten, G. Anticancer properties and mechanism of action of oblongifolin C, guttiferone K and related polyprenylated acylphloroglucinols. *Nat. Prod. Bioprospect.* **2021**, *11*, 629–641.
- (5) Espirito Santo, B. L. S. d.; Santana, L. F.; Kato Junior, W. H.; de Araújo, F. d. O.; Bogo, D.; Freitas, K. d. C.; Guimarães, R. d. C. A.; Hiane, P. A.; Pott, A.; Filiú, W. F. d. O.; Arakaki Asato, M.;

Figueiredo, P. d. O.; Bastos, P. R. H. d. O. Medicinal potential of *Garcinia* species and their compounds. *Molecules* **2020**, *25*, 4513.

(6) Klein-Júnior, L. C.; Campos, A.; Niero, R.; Corrêa, R.; Vander Heyden, Y.; Filho, V. C. Xanthones and cancer: from natural sources to mechanisms of action. *Chem. Biodiversity* **2020**, *17*, No. e1900499.

(7) Ye, Y. S.; Duan, Y. T.; Zhou, Z.; Thepkayson, K.; Douangdeuane, B.; Xu, G. Structurally diverse cytotoxic polyphenols from *Garcinia gracilis*. *J. Nat. Prod.* **2023**, *86*, 2206–2215.

(8) Supasuteekul, C.; Nonhitipong, W.; Tadtong, S.; Likhitwitayawud, K.; Tengamnuay, P.; Sritularak, B. Antioxidant, DNA damage protective, neuroprotective, and α -glucosidase inhibitory activities of a flavonoid glycoside from leaves of *Garcinia gracilis*. *Rev. Bras. Farmacogn.* **2016**, *26*, 312–320.

(9) Sukandar, E. R.; Kaennakam, S.; Raab, P.; Nöst, X.; Rassamee, K.; Bauer, R.; Siripong, P.; Ersam, T.; Tip-pyang, S.; Chavasiri, W. Cytotoxic and anti-inflammatory activities of dihydroisocoumarin and xanthone derivatives from *Garcinia picrorhiza*. *Molecules* **2021**, *26*, 6626.

(10) Sukandar, E. R.; Kaennakam, S.; Aree, T.; Nöst, X.; Rassamee, K.; Bauer, R.; Siripong, P.; Ersam, T.; Tip-pyang, S. Picrorhizone A–H, polyprenylated benzoylphloroglucinols from the stem bark of *Garcinia picrorhiza*. *J. Nat. Prod.* **2020**, *10*, 1–7.

(11) Zheng, D.; Jiang, J. M.; Chen, S. M.; Wan, S. J.; Ren, H. G.; Chen, G.; Xu, G.; Zhou, H.; Zhang, H.; Xu, H. X. Structural revision of guttiferone F and 30-epi-cambogin. *J. Nat. Prod.* **2021**, *84*, 1397–1402.

(12) Zheng, D.; Chen, Y.; Wan, S.; Jiang, J.; Chen, S.; Zheng, C.; Zhou, H.; Xu, G.; Zhang, H.; Xu, H. Polycyclic polyprenylated acylphloroglucinol congeners from *Garcinia yunnanensis* Hu with inhibitory effect on α -hemolysin production in *Staphylococcus aureus*. *Bioorg. Chem.* **2021**, *114*, 105074.

(13) Shan, W. G.; Lin, T. S.; Yu, H. N.; Chen, Y.; Zhan, Z. J. Polyprenylated xanthones and benzophenones from the bark of *Garcinia oblongifolia*. *Helv. Chim. Acta* **2012**, *95*, 1442–1448.

(14) Rubio, O. C.; Cuellar, A. C.; Rojas, N.; Castro, H. V.; Rastrelli, L.; Aquino, R. A polyisoprenylated benzophenone from Cuban propolis. *J. Nat. Prod.* **1999**, *62*, 1013–1015.

(15) Youn, U. J.; Sripisut, T.; Miklossy, G.; Turkson, J.; Laphookhieo, S.; Chang, L. C. Bioactive polyprenylated benzophenone derivatives from the fruits extracts of *Garcinia xanthochymus*. *Bioorg. Med. Chem. Lett.* **2017**, *27*, 3760–3765.

(16) Chien, S. C.; Chyu, C. F.; Chang, I. S.; Chiu, H. L.; Kuo, Y. H. A novel polyprenylated phloroglucinol, garcinialone, from the roots of *Garcinia multiflora*. *Tetrahedron Lett.* **2008**, *49*, S276–S278.

(17) Jia, C. C.; Xue, J. J.; Li, Z. L.; Li, D. H.; Hua, H. M. Antiproliferative polycyclic polyprenylated acylphloroglucinols from *Garcinia paucinervis*. *Nat. Prod. Res.* **2024**, *38*, 1687–1694.

(18) Pasaribu, Y. P.; Fadlan, A.; Fatmawati, S.; Ersam, T. Biological activity evaluation and in silico studies of polyprenylated benzophenones from *Garcinia celebica*. *Biomedicines* **2021**, *9*, 1654.

(19) Xu, Z. H.; Grossman, R. B.; Qiu, Y. F.; Luo, Y.; Lan, T.; Yang, X. W. Polycyclic polyprenylated acylphloroglucinols bearing a lavandulyl-derived substituent from *Garcinia xanthochymus* fruits. *J. Nat. Prod.* **2022**, *85*, 2845–2855.

(20) Marti, G.; Eparvier, V.; Moretti, C.; Prado, S.; Grellier, P.; Hue, N.; Thoison, O.; Delpech, B.; Guéritte, F.; Litaudon, M. Antiplasmodial benzophenone derivatives from the root barks of *Symphonia globulifera* (Clusiaceae). *Phytochemistry* **2010**, *71*, 964–974.

(21) *Molecular Operating Environment (MOE) version 2009.10*; Chemical Computing Group, Inc.: Montreal (QC) Canada, 2009.

(22) Bruhn, T.; Schaumlöffel, A.; Hemberger, Y.; Bringmann, G. SpecDis: Quantifying the comparison of calculated and experimental electronic circular dichroism spectra. *Chirality* **2013**, *25*, 243–249.

(23) Grimblat, N.; Zanardi, M. M.; Sarotti, A. M. Beyond DP4: an improved probability for the stereochemical assignment of isomeric compounds using quantum chemical calculations of NMR shifts. *J. Org. Chem.* **2015**, *80*, 12526–12534.

(24) Sarotti, A. M.; Pellegrinet, S. C. A multi-standard approach for GIAO ^{13}C NMR calculations. *J. Org. Chem.* **2009**, *74*, 7254–7260.

(25) Sarotti, A. M.; Pellegrinet, S. C. Application of the multi-standard methodology for calculating ^1H NMR chemical shifts. *J. Org. Chem.* **2012**, *77*, 6059–6065.

(26) Frisch, M. J.; Trucks, G. W.; Schlegel, H. B.; Scuseria, G. E.; Robb, M. A.; Cheeseman, J. R.; Scalmani, G.; Barone, V.; Petersson, G. A.; Nakatsuji, H.; Li, X.; Caricato, M.; Marenich, A. V.; Bloino, J.; Janesko, B. G.; Gomperts, R.; Mennucci, B.; Hratchian, H. P.; Ortiz, J. V.; Izmaylov, A. F.; Sonnenberg, J. L.; Williams-Young, D.; Ding, F.; Lipparini, F.; Egidi, F.; Goings, J.; Peng, B.; Petrone, A.; Henderson, T.; Ranasinghe, D.; Zakrzewski, V. G.; Gao, J.; Rega, N.; Zheng, G.; Liang, W.; Hada, M.; Ehara, M.; Toyota, K.; Fukuda, R.; Hasegawa, J.; Ishida, M.; Nakajima, T.; Honda, Y.; Kitao, O.; Nakai, H.; Vreven, T.; Throssell, K.; Montgomery, J. A., Jr; Peralta, J. E.; Ogliaro, F.; Bearpark, M. J.; Heyd, J. J.; Brothers, E. N.; Kudin, K. N.; Staroverov, V. N.; Keith, T. A.; Kobayashi, R.; Normand, J.; Raghavachari, K.; Rendell, A. P.; Burant, J. C.; Iyengar, S. S.; Tomasi, J.; Cossi, M.; Millam, J. M.; Klene, M.; Adamo, C.; Cammi, R.; Ochterski, J. W.; Martin, R. L.; Morokuma, K.; Farkas, O.; Foresman, J. B.; Fox, D. J. *Gaussian 16*, Rev. C.01; Gaussian, Inc.: Wallingford (CT) USA, 2016.